Proteomic and Lipidomic Plasma Evaluations Reveal Biomarkers for Domoic Acid Toxicosis in California Sea Lions

Amie M. Solosky[1], Iliana M. Claudio[2], Jessie R. Chappel[3], Kaylie I. Kirkwood-Donelson[4], Michael G. Janech[5], Alison M. Bland[5], Frances M.D. Gulland[6], Benjamin A. Neely[7], and Erin S. Baker[1*]*

[1]Department of Chemistry, University of North Carolina at Chapel Hill, Chapel Hill, NC, USA

[2]Department of Chemistry, North Carolina State University, Raleigh, NC, USA

[3]Department of Biological Sciences, North Carolina State University, Raleigh, NC, USA

[4]Immunity, Inflammation, and Disease Laboratory, National Institute of Environmental Health Sciences, Durham, NC, USA

[5]Department of Biology, College of Charleston, Charleston, SC, USA

[6]Wildlife Health Center, University of California, Davis, CA, USA

[7]Chemical Sciences Division, National Institute of Standards and Technology, Charleston, SC, USA

* Correspondence: Co-corresponding Authors
benjamin.neely@nist.gov, erinmsb@unc.edu

ABSTRACT

Domoic acid is a neurotoxin secreted by the marine diatom genus, *Pseudo-nitzschia,* during toxic algal bloom events. California sea lions (*Zalophus californianus*) are exposed to domoic acid through ingestion of fish that feed on toxic diatoms, resulting in a domoic acid toxicosis (DAT), which can vary from mild to fatal. Sea lions with mild disease can be treated if toxicosis is detected early after exposure, therefore, rapid diagnosis of DAT is essential but also challenging. In this work, we performed multi-omics analyses, specifically proteomic and lipidomic, on blood samples from 31 California sea lions. Fourteen sea lions were diagnosed with DAT based on clinical signs and postmortem histological examination of brain tissue, and 17 had no evidence of DAT. Proteomic analyses revealed three apolipoproteins with statistically significant lower abundance in the DAT individuals compared to the non-DAT individuals. These proteins are known to transport lipids in the blood. Lipidomic analyses highlighted 29 lipid levels that were statistically different in the DAT versus non-DAT comparison, 28 of which were downregulated while only one was upregulated. Furthermore, of the 28 downregulated lipids, 15 were triglycerides, illustrating their connection with the perturbed apolipoproteins and showing their potential for use in rapid DAT diagnoses.

KEYWORDS

Domoic Acid, Proteomics, Lipidomics, California Sea Lion, Zalophus californianus, Ion Mobility Spectrometry, Multi-omics

SYNOPSIS

Multi-omics evaluations reveal blood apolipoproteins and triglycerides are altered in domoic acid toxicosis in California sea lions.

GRAPHIC ABSTRACT

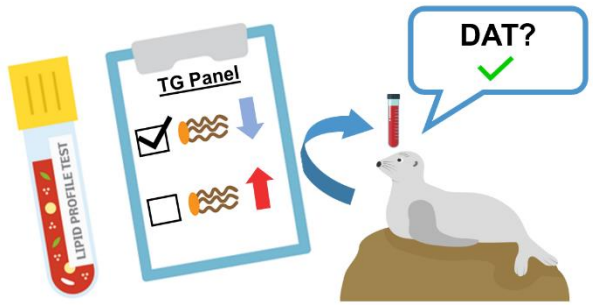

INTRODUCTION

Domoic acid is a naturally occurring toxin produced by the pennate diatom, *Pseudo-nitzschia*[1], a harmful algal bloom that is increasing in frequency and extent along the U.S. west coast.[2] In birds and mammals, domoic acid acts as an excitotoxin, affecting the brain and causing permanent short-term memory loss, seizures, brain damage, and death in certain situations.[3, 4] Specifically, exposure to domoic acid results in domoic acid toxicosis (DAT) in California sea lions (*Zalophus californianus)* and other animals such as seabirds and even humans.[3,5,6] More specifically, sea lions are exposed to domoic acid through anchovies and sardines in their diet that accumulate the toxin from eating and swimming in the algae (**Figure 1**).[7] Following exposure, domoic acid binds to glutamate receptors in the sea lion's brain causing neurological dysfunction including seizures and

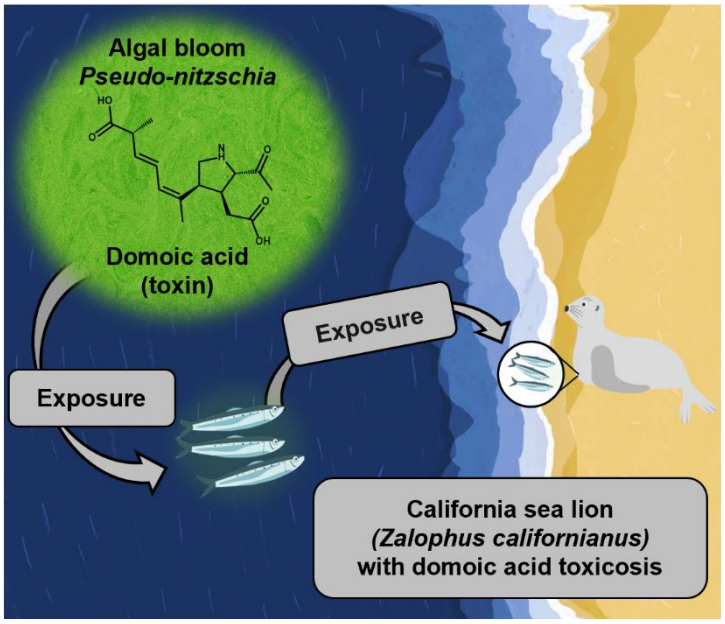

Figure 1. California sea lion domoic acid exposure routes. First, *Pseudo-nitzschia* secretes domoic acid during algal blooms. The domoic acid is then accumulated in fish due to their diet of zooplankton that feed on algal cells, or the diatoms themselves. Finally, sea lions are exposed when eating contaminated fish. Depending on the amount of domoic acid present, this exposure can cause toxicosis, which can be fatal.

65 ataxia.[8] Additionally, the toxin can bind to receptors in the heart, giving rise to cardiomyopathy
66 and fatality.[3]

67 DAT has been impacting sea lions for over 25 years, causing them to strand on beaches and
68 need immediate medical attention.[5,6] In 1998, it was estimated that The Marine Mammal Center
69 (Sausalito, CA) rescued 400 sea lions, with at least 70 experiencing seizures, head weaving, or
70 even unresponsiveness (coma) from DAT.[6,7] Between 1998 and 2019, over 11,000 California sea
71 lions have been admitted to TMMC and evaluated for DAT.[6] Additionally, the annual rate of DAT
72 in sea lions is expected to continue rising based on the 2.1 % increase per year between 1998 and
73 2019.[6] More concerningly, the rapid diagnosis of DAT is challenging since domoic acid is rapidly
74 metabolized and not detected in urine or blood greater than 24 hours post exposure.[6] Current
75 diagnostic approaches include examining clinical signs such as behavioral changes (seizures,
76 coma, ataxia), antemortem MRIs, blood eosinophil cell counts, and histological samples of the
77 brain postmortem.[6] While these methods have been successful, they are not specific, and require
78 highly trained technicians and anesthesiologists. Furthermore, some can only be performed
79 postmortem.[6] Despite diagnosis being a challenge, treatment for DAT in sea lions does differ than
80 other ailments, for example, an individual suffering from DAT may be administered anti-seizure
81 medications as well as supportive subcutaneous fluids to induce flushing of the toxin out of the
82 body.[6] Thus, evaluating potential molecular biomarkers that can be found in blood samples taken
83 while the animal is alive and at early stages of DAT would facilitate effective treatment and reduce
84 DAT-associated mortality.

85 Multi-omic analyses are a promising approach for DAT biomarker evaluation, as they reveal
86 molecular changes, such as protein and lipid changes, specific to DAT over other ailments.[9,10]
87 Proteomic analyses of California sea lion plasma and cerebral spinal fluid were performed in 2015,

88 resulting in 20 potential protein biomarkers for DAT with seven proteins upregulated in sea lion
89 cerebral spinal fluid and apolipoprotein E downregulated in plasma.[11,12] Here we performed
90 another proteomic assessment of sea lion plasma for 31 California sea lions (14 DAT and 17 non-
91 DAT) due to the recent release of a new sea lion genome and newer mass spectrometry
92 instrumentation. Additionally, due to previous detection of alteration of apolipoprotein E,[12] we
93 added lipidomic analyses to further evaluate molecular alterations in DAT and assess potential
94 biomarkers for better diagnosis of California sea lions.

95

96 **MATERIALS AND METHODS**

97 ***Sea Lion Blood Sample Collection, Preparation, and Inclusion & Exclusion Criteria***

98 The California sea lion plasma was collected between 2007 and 2012, near or at their time of
99 admission to The Marine Mammal Center (TMMC) in Sausalito, CA, following rescue due to
100 numerous illnesses[12]. The TMMC Internal Animal Care and Use Committee approved protocols
101 for this study (number 2007–2), and the research was conducted under the National Fisheries
102 Service MMPA permit numbers 932-1489-00 and 932-1905-00. Data analysis was approved under
103 NIST Research Protections Office (RPO) approval MML-AR20-0001. After collection, blood was
104 placed in Na-citrate tubes, centrifuged at 3,000 rpm for 10 min, and the plasma layer was
105 transferred to a cryovial and stored at -80 °C within 2 h. Thirty-one California sea lion samples
106 were selected for the proteomic and lipidomic analyses due to their DAT and non-DAT statuses
107 as defined by Neely et al.[12] Of these, fourteen of the individuals were diagnosed with DAT and
108 the seventeen remaining had other ailments such as leptospirosis or were suffering from
109 malnutrition. The hematological and individual characteristics of each animal are provided in
110 **Table S1** and **Table S2**.

111

112 ***Chemicals and Reagents***

113 All chemical reagents unless otherwise stated were purchased from ThermoFisher Scientific
114 (Waltham, MA). For specific catalog numbers for all chemicals, reagents, and equipment, see
115 **Table S3**.

116

117 ***Proteomic Sample Preparation***

118 Prior to the study, the 31 sea lion plasma samples were randomized and assigned an
119 experimental key to avoid bias and minimize batch effects. Each sample was then thawed and
120 centrifuged at 13 000 x g_n for 8 min at 4 °C. Based on prior work with California sea lion and other
121 mammalian plasma, a protein concentration of approximately 50 µg/µL was assumed for
122 estimating the amount of enzyme for digestion. Therefore, 2 µL (approximately 100 µg protein)
123 of each sample was added to 78 µL of 50 mmol/L ammonium bicarbonate buffer in water in Lo-
124 Bind microcentrifuge tubes (Eppendorf; Hamburg, Germany); these aliquots from each sample
125 were briefly mixed by vortexing and immediately used for digestion. Simultaneously, a pool was
126 generated using 5 µL aliquots from each sample. The pool was digested in parallel to the individual
127 samples and later used as a technical replicate during the LC-MS/MS analysis (**Figure 2A**).
128 Proteins were reduced with 9 µL of 90 mmol/L DL-Dithiothreitol (DTT; final concentration of 9
129 mM) at 60 °C for 30 min, then cooled and alkylated with 9 µL of 200 mmol/L 2-chloroacetamide
130 (CAA; final concentration of 18 mM) at room temperature in the dark for 30 min. An additional
131 100 µL of 50 mmol/L ammonium bicarbonate was added prior to enzymatic digestion. First, LysC
132 (Thermo Scientific; Waltham, MA) was added at a 1:100 mass ratio (LysC:total protein) ratio,
133 using 2 µL of a 0.5 µg/µL solution, and incubated at 37 °C for 1 h. Next, trypsin (Pierce Trypsin

134 Protease, Thermo Scientific; Waltham, MA) was added at a 1:20 mass ratio (trypsin:total protein)
135 using 5 μL of 1 μg/μL solution. Samples were incubated at 37 °C for 4 h, after which the reaction
136 was halted by adding 5 μL of 4 % formic acid (volume fraction). Peptide samples were purified
137 for LC-MS/MS using Pierce C18 spin columns (8 mg C18 resin) according to the manufacturer's
138 instructions. Briefly, 0.5 % trifluoroacetic acid (volume fraction) in 5 % acetonitrile (volume
139 fraction) was used for wash steps, while 60 μL of 70 % acetonitrile (volume fraction) was used for
140 elution. The samples were reduced to dryness in a vacuum centrifuge at low heat and stored at -20
141 °C. Samples were then reconstituted with 100 μL of 0.1 % formic acid (volume fraction), vortexed
142 for 10 min, and the Pierce quantitative fluorometric peptide assay was used to determine sample

143 peptide concentrations with a BioTek Synergy HT plate reader (Agilent Technologies; Santa Clara,

144 CA).

145 ***Proteomic nanoLC-MS/MS Instrumentation***

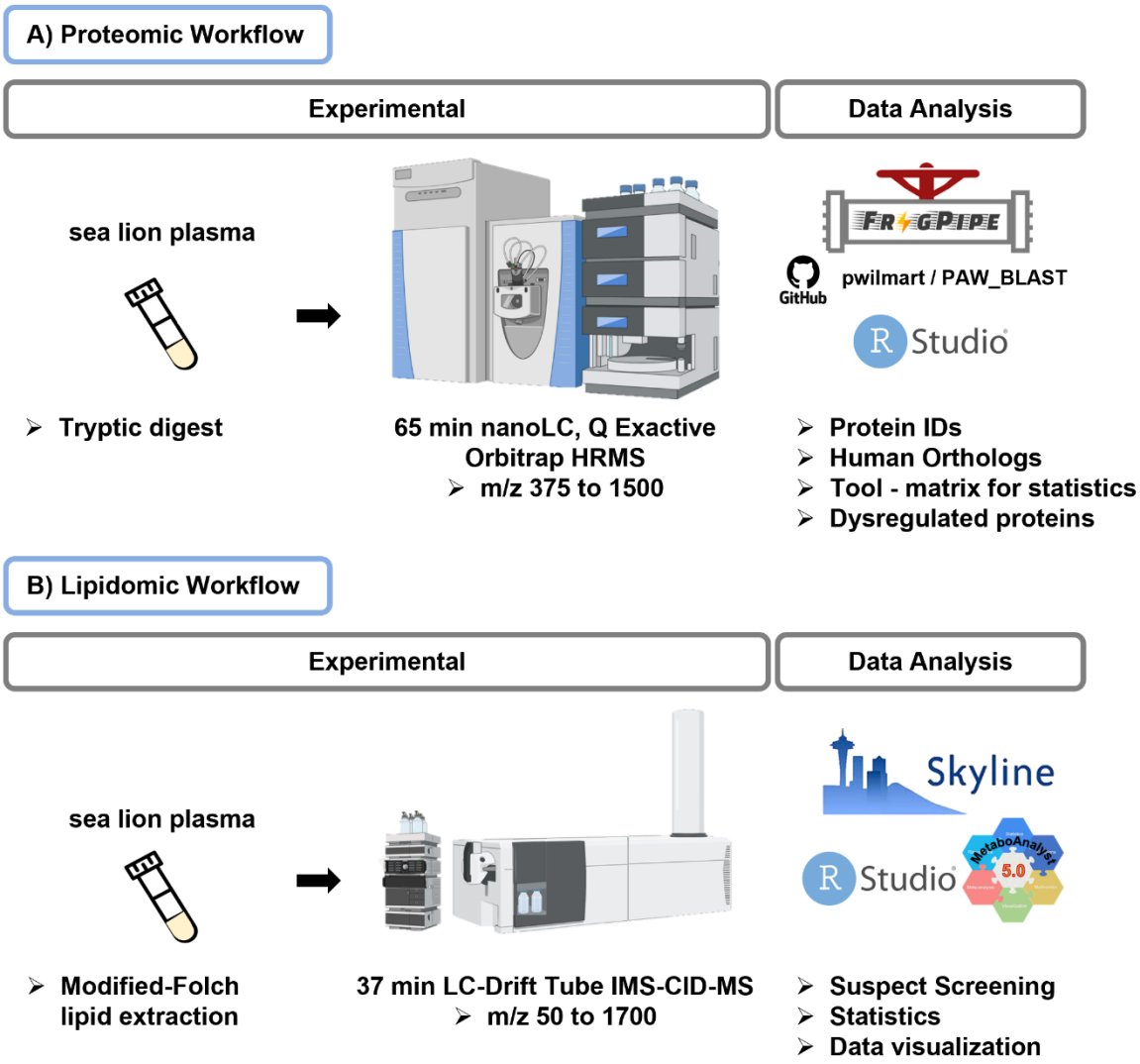

Figure 2. Proteomic and lipidomic sample workflows. **A)** For the proteomic workflow, a tryptic digest of sea lion was separated with nanoflow liquid chromatography and data acquired with a Q Exactive orbitrap mass spectrometer. Data was searched with FragPipe and analyzed in R. **B)** The lipidomic workflow consisted of a modified-Folch lipid extraction of the plasma, followed by LC-IMS-CID-MS analysis. Lipidomic data sets were processed using Skyline software with in-house libraries containing over 1,000 lipids with LC retention time, CCS, and *m/z* values for each. Statistics and data visualization were performed using MetaboAnalyst 6.0 and RStudio. The figure was created with BioRender.

146 Peptide mixtures in 0.1 % formic acid (volume fraction) were analyzed using an UltiMate 3000
147 nanoLC coupled to a Q Exactive Orbitrap mass spectrometer (Thermo Fisher Scientific; Waltham,
148 MA). Peptide mixtures were loaded onto a PepMap 100 C18 trap column (75 µm id x 2 cm length;
149 Thermo Fisher Scientific; Waltham, MA) at 3 µL/min for 10 min with 2 % acetonitrile (volume
150 fraction) and 0.05 % trifluoroacetic acid (volume fraction) followed by separation on an Acclaim
151 PepMap RSLC 2 µm C18 column (75µm id x 25 cm length; Thermo Fisher Scientific; Waltham,
152 MA) at 40 °C. A randomized sample order and injection volumes were determined for 1 µg loading
153 (between 2.8 µL and 7.7 µL). Peptides were separated along a 65 min gradient with mobile phase
154 A (MPA) consisting of 0.1 % formic acid (volume fraction) in water and mobile phase B (MPB)
155 being 80 % acetonitrile (volume fraction) and 0.08 % formic acid (volume fraction) in water. A
156 two-step gradient was used, beginning with 5 % to 30 % MPB over 50 min followed by 10 min
157 ramp to 45 % MPB, and lastly to 95 % MPB over 5 min, and held at 95 % MPB for 5 min, all at a
158 flow rate of 300 nL/min. The Fusion Lumos was operated in positive polarity with 30 % RF lens,
159 data-dependent mode (topN, 3 sec cycle time) with a dynamic exclusion of 60 s (with 10 ppm
160 error). Full scan resolution using the orbitrap was set at 60 000, the mass range was *m/z* 375 to
161 1500. The full scan ion target value was 4.0 x 10^5 allowing a maximum injection time of 50 ms.
162 Monoisotopic peak determination was used, specifying peptides and an intensity threshold of 2.5
163 x 10^4 was used for precursor selection, including charge states 2 to 6. Data-dependent
164 fragmentation was performed using higher-energy collisional dissociation (HCD) at a normalized
165 collision energy of 32 with quadrupole isolation at *m/z* 1.3 width. The fragment scan resolution
166 using the orbitrap was set at 15 000 for *m/z* 100 as the first mass, ion target value of 2.0 x 10^5, and
167 30 ms maximum injection time. The MS1 data was collected as profile data, while the MS2 data
168 was collected as centroid data. The function, inject all ions for parallelizable time, was not used in

169 the analysis. The raw data and tissue specific search results along with all databases used are
170 available at the ProteomeXchange Consortium[13] via the PRIDE partner repository with the dataset
171 identifiers PXD020366 and 10.6019/PXD020366.[14]
172
173 ***Protein Identification and Label-free Quantification***
174 The data-dependent acquisition data was searched with FragPipe (v20.0), a software package
175 that includes the MSFragger search algorithm (v3.8),[15] Philosopher protein inference model
176 (v5.0.0),[16] and an IonQuant label-free quantification algorithm (v1.9.8).[17] The parameter file used
177 (which can be viewed and loaded into FragPipe) is also available as supplemental **File S1**. The
178 search parameters were chosen for trypsin and LysC, and it is known that non-specific enzyme
179 activity occurs in biofluids. Broadly, the parameters included semitryptic cleavage with a strict
180 trypsin cleavage rule (cut after KR) and allowing for two mis-cleavages. The precursor and
181 fragment mass tolerances were initially set to 20 ppm for precursor and fragment mass tolerance,
182 though MSFragger runs a mass calibration and optimization step to set these tolerances
183 automatically. Oxidized methionine, protein n-term acetylation, and peptide n-term pyroGlu were
184 allowed as variable modifications and carbamidomethylation of cysteine was a fixed modification.
185 The LFQ-MBR (label-free quantification match between runs) workflow was used, which is
186 IonQuant-based MS1 quantification with match between runs. The built-in FragPipe function of
187 fasta selection was used to select the UniProtKB *Zalophus californianus* (California sea lion; taxon
188 ID 9704) proteome UP000515165 (47 492 sequences; retrieved 8 August 2023). This proteome is
189 based on an updated NCBI RefSeq annotation that used the 2020 Vertebrate Genome Project
190 Genome mZalCal1.pri.v2 assembly, but still used the underlying RNAseq data previously
191 deposited[18]. Using FragPipe, 118 contaminant sequences (such as human keratin or porcine

192 trypsin) were added, and finally the fasta was concatenated with reverse entries (95,230 entries
193 total).
194
195 ***Protein Ortholog Mapping***

196 The UniProtKB *Zalophus californianus* (California sealion; taxon ID 9704) proteome
197 UP000515165 contained mostly gene symbol IDs, therefore there was not a drastic need to perform
198 orthology mapping on all 485 initially identified proteins (note some without quantification, see
199 below). Instead, only 71 of the identified proteins were missing gene symbols and had locus
200 numbers (ex. LOC118356106 for serum amyloid protein A). Human orthologs were assigned to
201 these 71 proteins using a series of python scripts (Anaconda v2023.07; conda v23.5.2; Python
202 v3.8.17) from Github on the following two repositories: pwilmart/PAW_BLAST and
203 pwilmart/annotations, retrieved October 12, 2021. First, the 71 identifiers in question were used to
204 create a subset fasta (make_subset_DB_from_list_3.py), which was then searched against a human
205 fasta [UniProtKB *Homo sapiens* (Human; taxon ID 9606) canonical proteome UP000005640;
206 2023_03 release] using the db_to_db_blaster.py script, which used a local installation of BLAST+
207 2.11.0. This list was manually confirmed by comparing sea lion to human ortholog protein names,
208 and when needed, running BLAST with sea lion entries against all mammals. Incorrect
209 assignments can happen when a protein is not present in humans (e.g., beta-lactoglobulin 1;
210 UniProtKB A0A6P9EXQ1), or if the human BLAST hit disagrees with the original annotation, in
211 which case the original annotation is preserved (e.g., sea lion haptoglobin was matched to human
212 haptoglobin-related protein, but we kept the original name of haptoglobin and the HP symbol).
213 Once all 485 identified sea lion proteins had gene symbols, any proteins with all zeros by MaxLFQ
214 intensity were removed (this can occur when a tandem mass spectrum is identified in FragPipe,

215 but a quantity not calculated). Next, any remaining duplicate gene symbol entries were summed
216 together into a single nonredundant entry. This resulted in 245 proteins identified experiment-
217 wide, which were used for statistical testing (**Table S5**).

218

219 ***Proteomic Statistical Data Analysis***

220 A two-sided Wilcoxon rank sum test (equivalent to the Mann-Whitney U-test) was used to
221 detect statistically significant proteins. This was performed with R (v4.2.0) and the dplyr package
222 (v1.1.0) using the *wilcox.test* function and p-value correction with the Benjamini and Hochberg
223 method, using the *p.adjust* function specifying 'BH'.[19] Proteins with adjusted $p < 0.05$ (*i.e.,* FDR
224 < 0.05) were deemed significantly different.[19] Since zeros cannot be used to calculate fold-change,
225 all zeros were replaced with ½ the lowest observed non-zero value for each given protein. This
226 imputation did not affect rank sum statistics but is used solely to provide a reference for protein
227 change between groups.

228

229 ***Lipidomic Sample Preparation***

230 For the lipidomic analyses, lipids from the 31 individual plasma samples, as well as four pooled
231 samples, were extracted using a modified-Folch extraction.[20] This lipid extraction method was
232 previously described and validated by Kirkwood et al., using NIST SRM 1950 (metabolites in
233 frozen human plasma) as a quality control to compare with other extraction methods.[22] The
234 modified-Folch extraction resulted in a comparable amount of lipids, as well as category
235 compositions, as various other extraction methods performed by the LIPID MAPS consortium.[22]
236 See **Figure 2B** for the lipidomic workflow used in the present study. Briefly, 50 µL of plasma was
237 transferred into a 1.7 mL Sorensen SafeSeal™ Microcentrifuge tube (Waltham, MA) with 600 µL

238 of 2:1 (volume ratio) chloroform/LC-MS grade methanol at -20 °C. Each sample was vortexed for
239 30 s at 1200 rpm using a Digital Vortex Mixer (Thermo Scientific; Waltham, MA) and then 150
240 µL of LC-MS grade water was added, prior to mixing again for 30 s. The samples were then left
241 at room temperature for 5 min to allow adequate time for phase separation, centrifuged at 12 000
242 rpm for 10 min at 4 °C for further phase separation, and immediately placed on ice to prevent
243 degradation.[21] Since this liquid/liquid extraction results in both a top (aqueous) and bottom
244 (organic) extraction layer, 100 µL of the bottom layer was aliquoted into a new tube and dried
245 down using a SpeedVac vacuum concentrator (ThermoFisher Scientific; Waltham, MA).
246 Following dry down, the lipid extract was immediately reconstituted in 10 µL of chloroform and
247 190 µL of LC-MS grade methanol. The samples were stored in 2-mL amber glass LC autosampler
248 vials (Agilent Technologies; Santa Clara, CA) at -20 °C until analysis (less than 1 week). The
249 lipidomic pooled quality control sample was made by combining equal amounts of each individual
250 sample into a new 1.7 mL Sorensen SafeSeal™ Microcentrifuge tube (Sorensen Bioscience, Inc.;
251 Murray, UT). The pool was then vortexed for 30 s and underwent the same modified-Folch
252 extraction steps as above in parallel with the rest of the sample set. The final QC sample was split
253 into four vials to provide technical replicates for the LC-IMS-CID-MS analyses.

254 ***Lipidomic LC-IMS-CID-MS Instrumentation***

255 Lipidomic analyses of the 31 plasma samples were performed using a previously described
256 untargeted platform combining liquid chromatography, ion mobility spectrometry, collision-
257 induced dissociation, and mass spectrometry (LC-IMS-CID-MS).[22] **Figure 2B** illustrates the
258 lipidomic workflow. These separations were performed on an Agilent 1290 Infinity UPLC system
259 (Agilent Technologies; Santa Clara, CA) coupled to an Agilent 6560 IM-QTOF platform (Agilent
260 Technologies; Santa Clara, CA) with a commercial gas kit and a MKS Instruments precision flow

controller (Andover, MA).[22] Prior to all lipidomic studies, Agilent ESI-L Low Concentration tuning mix solution (Agilent Technologies; Santa Clara, CA) was injected in the 6560 IM-QTOF platform to verify mass accuracy and collision cross section (CCS) values of the platform. Brain total lipid extract standard (Avanti Polar Lipids; Alabaster, AL) was run prior to samples to assess lipidomic separations and quality. Then, 10 µL of each individual plasma lipid extract was injected onto a Waters Acquity UPLC CSH^{TM} C18 column (Milford, MA) (3.0 mm x 150 mm x 1.7 µm particle size), where MPA was comprised of 40:60 (volume ratio) LC-MS grade ACN/H_2O and 10 mmol/L ammonium acetate and MPB consisted of 90:10 (volume ratio) LC-MS grade IPA/ACN with 10 mmol/L ammonium acetate. The 34 min LC gradient had a constant flow rate of 0.25 mL/min and time to MPB ratio as follows [time (min):MPB (%; volume fraction to MPA)): 0:40, 2:50, 3:60, 12:70, 15:75, 17:78, 19:85, 22:92, 25:99, and 34:99]. The gradient was followed by a 3 min column wash step as follows [flow rate (mL/min): time (min):MPB (%; volume fraction to MPA)): 0.30:34.5:40, 0.30:35:99, 0.30:35.5:99, 0.35:36:40, 0.30:37:40, and 0.25:38:40]. For the IMS-MS analyses, the Agilent Jet Stream ESI source was utilized, and the platform was operated in both negative and positive ionization modes. For the IMS analyses, the funnel trap fill time was set to 10 ms with a release time of 400 µs. Following drift time separation, the CID analysis consisted of a data-independent approach where lipid ions were fragmented using a CID ramp based on the precursor ion's drift time (**Table S4)**. Finally, a quadrupole time-of-flight (QTOF) mass spectrometer evaluated ion from 50 to 1700 *m/z*, and a .d file was collected containing the multidimensional LC, IMS, CID, and MS information.

The .d LC-IMS-CID-MS data files were then single-field calibrated to calculate CCS values for all lipids in the samples using the Agilent MassHunter Workstation Software IM-MS Browser Version B.10.00 and the previously mentioned Agilent tuning mix.[23] All raw data files were

284 evaluated using Skyline software, an open source, non-vendor specific software to process various
285 types of mass spectrometry data (MacCoss Lab Software, v. 22.2).[24,25] In Skyline, lipids were
286 annotated based on how closely the extracted ion chromatograms matched our in-house spectral
287 lipid library, which contained 877 lipids and is publicly available at
288 https://tarheels.live/bakerlab/databases/.[22,26] The parameters manually assessed were retention
289 time index, *m/z* values with a mass error of less than 5 ppm, and CCS values within the resolving
290 power window of 50.[26] Peaks were additionally validated by precursor isotope distribution and
291 fragmentation spectra. The raw data is available on Panorama at
292 https://panoramaweb.org/sealionlipids.url.
293
294 ***Lipidomic Statistical Analysis***
295 The list of lipid identifications and their corresponding peak areas in the samples from Skyline
296 were then normalized via total ion current and $\log_2$ transformed. The normalized and transformed
297 peak areas were imported into MetaboAnalyst 6.0 to assist in data visualization using hierarchical
298 clustering (based on Euclidean distances) in the form of a heatmap to assess differences between
299 the DAT and non-DAT sea lions.[27] Additional statistical analyses were also performed using
300 RStudio (R version 4.3.1) including the following packages: dplyr and Lipid Mini-On (rodin).[19,28]
301 In the same fashion as the proteomic statistical analysis, the lipidomic statistical comparisons
302 included a two-sided Wilcoxon rank sum test and fold change comparisons. Additionally, volcano
303 plots and bar charts were used for data visualization.
304
305 **RESULTS & DISCUSSION**
306 ***Proteomic Analyses***

307 In the proteomic analyses of the 31 plasma samples, 245 proteins were identified from 9079
308 peptides (**Table S5**) and statistical assessments of the DAT versus non-DAT groups found 31
309 proteins were statistically significant (Benjamini-Hochberg adjusted p-value < 0.05, **Table S7**).
310 Of these proteins, three were apolipoproteins (APO): APOC3, APOE, and APOB (noted with * in
311 **Figure 3**) and an additional eight apolipoproteins were also detected with specific trends. Since
312 APOE was observed to be of statistical significance and decreased in this sample previously using
313 2D-gel, its results were not surprising.[12] However, APOC3 downregulation in DAT individuals
314 was of great interest as its high levels have been linked to hypertriglyceridemia in humans,
315 indicating a potential for hypotriglyceridemia in the DAT group.[29] Downregulation of APOB has
316 also been linked with decreased triglyceride availability in humans, and as the protein plays a role
317 in lipid metabolism, this further illustrates the need for a lipidomics assessment.[30] Additionally, of

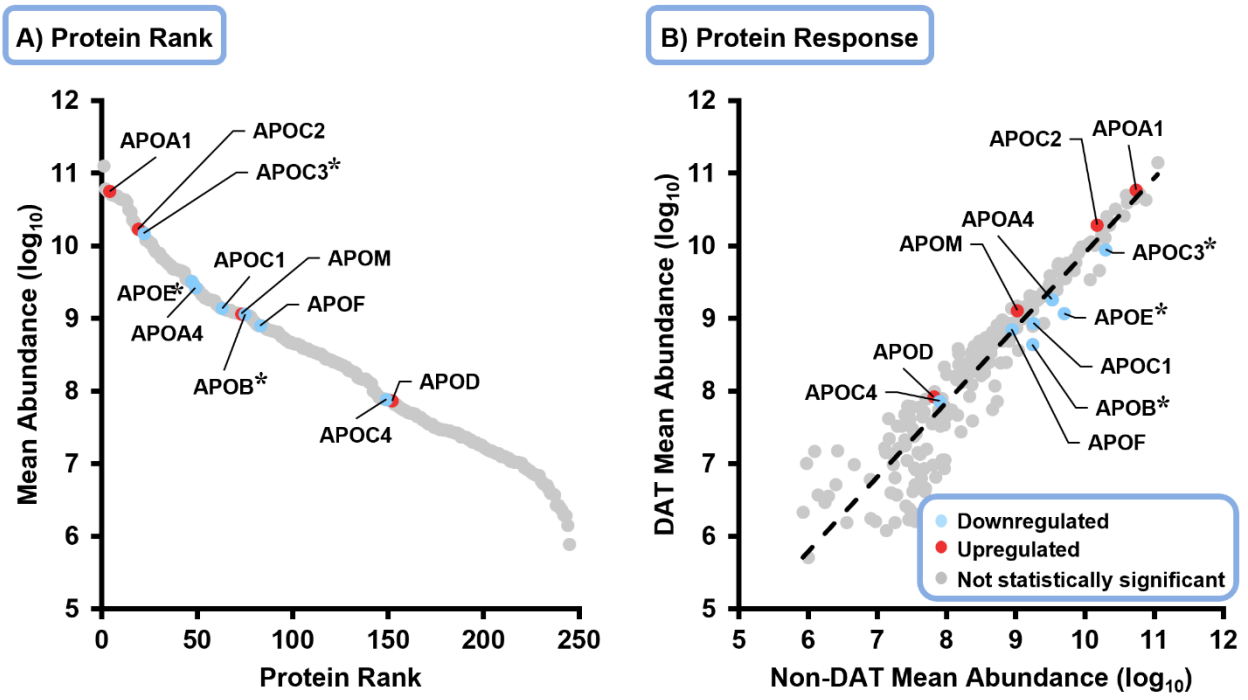

Figure 3. Eleven apolipoproteins detected in the sea lion proteomic analyses and illustrated in **A)** rank abundance and **B)** protein response graphs. Apolipoproteins are highlighted in either red or blue, indicating up (red) or downregulation (blue), while all other detected proteins are shown in grey. The dashed line in **B)** represents a 1:1 reference, where proteins above are upregulated and below are downregulated. The statistically significant apolipoproteins are noted with asterisks.

318 the 11 apolipoproteins detected in this study while eight were not statistically significant they did
319 have interesting trends. For example, APOC1 and APOC4 had lower abundances in the DAT
320 group and are thought to be involved in triglyceride metabolism, although the function of
321 endogenous APOC4 is not completely known.[31,32] APOC2 was also not statistically significant but
322 trended higher in the DAT group, and high APOC2 levels have been associated with
323 downregulation of plasma TGs in humans.[32] Since this study size is small, the trends in these non-
324 significant apolipoproteins are also notable.

325 Of the other 28 proteins found to be statistically significant altered in DAT in the study, other
326 interesting trends were observed and angiopoietin-like 3 (ANGPTL3), hepatocyte growth factor
327 activator (HGFA), coagulation factor XII, and CD5 antigen-like protein (CD5L) were of particular
328 interest. For example, ANGPTL3 had the lowest $\log_2$ fold change (approximately -4) out of all the
329 significant proteins and is involved in blood TG regulation.[33] HGFA and coagulation factor XII,
330 which were higher in DAT individuals, are both proteases thought to activate hepatocyte growth
331 factor signaling,[34] a signaling pathway activated when there is injury to tissues.[34] Furthermore,
332 coagulation factor XII has been linked to pro-inflammatory cytokines in antigen-presenting cells
333 in atherosclerosis-prone mice, indicating an increased immune response,[35] which could help
334 explain why sea lions with DAT may suffer from cardiomyopathy. Lastly, CD5L, which was
335 downregulated in the DAT individuals, is involved in lipid homeostasis and immunomodulation.
336 Additionally, it has been linked to mediate autoimmunity by altering fatty acid composition and
337 inhibiting cholesterol biosynthesis.[36,37] Thus, in addition to the apolipoproteins, all four of these
338 proteins of interest have been linked to lipids and further support our hypothesis that lipids are
339 dysregulated in individuals with DAT.
340

341 ***Lipidomics Analyses***

342 In the lipidomic analyses of the 31 sea lion plasma samples, 331 unique lipids in five lipid
343 categories (fatty acyl, sterol, glycerolipid, glycerophospholipid, and sphingolipid) were identified
344 at a Schymanski confidence level of 2 or 3.[22,26,38] Of the identified lipids, 29 were found to be
345 statistically significant in the DAT versus non-DAT comparison, with 28 downregulated and 1
346 upregulated (**Table S8**). Moreover, while the statistically significant lipids span four out of the
347 five lipid categories assessed, 15 of the 29 were triglycerides (TGs), illustrating their potential link
348 to DAT and its apolipoprotein dysregulation. In general, the glycerolipids (TGs and diglycerides
349 (DGs)) were remarkably enriched, making up just 15 % of all 331 detected lipids and 55 % of the
350 significant. Furthermore, all but one of the significant lipids were lower in the DAT sea lion

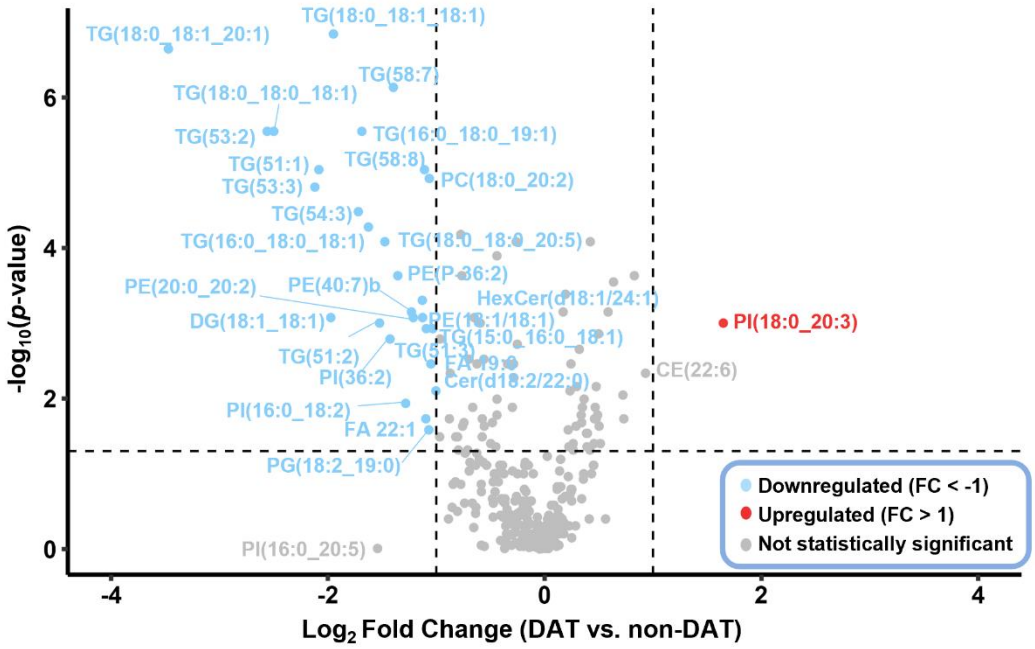

Figure 4. Lipids detected and dysregulated in the DAT versus non-DAT California sea lion plasma comparison. Blue data points show downregulated lipids, red show upregulated, and grey show those not statistically significant in the comparison. Of the significant lipids, 50 % are triglycerides. The full list of significant lipids is included in **Table S8**.

351 plasma, including all TGs as shown in the volcano plot in **Figure 4**. The single upregulated

352 significant lipid was a phosphatidylinositol species (PI(18:0_20:3)). Interestingly,
353 phosphatidylinositols are precursors for DGs, which is another glycerolipid like TGs but with one
354 less fatty acyl chain.[39] This is worth noting because one diglyceride, DG(18:1_18:1), was found to
355 be downregulated and statistically significant in the DAT individuals, which indicates that a lack
356 of DG(18:1_18:1) synthesis may a consequence when a higher abundance of PI(18:0_20:3) is
357 observed due to the PI not being converted to a DG, but requires more investigation.

358 To further evaluate the lipidomic changes in DAT individuals, the significant lipids were

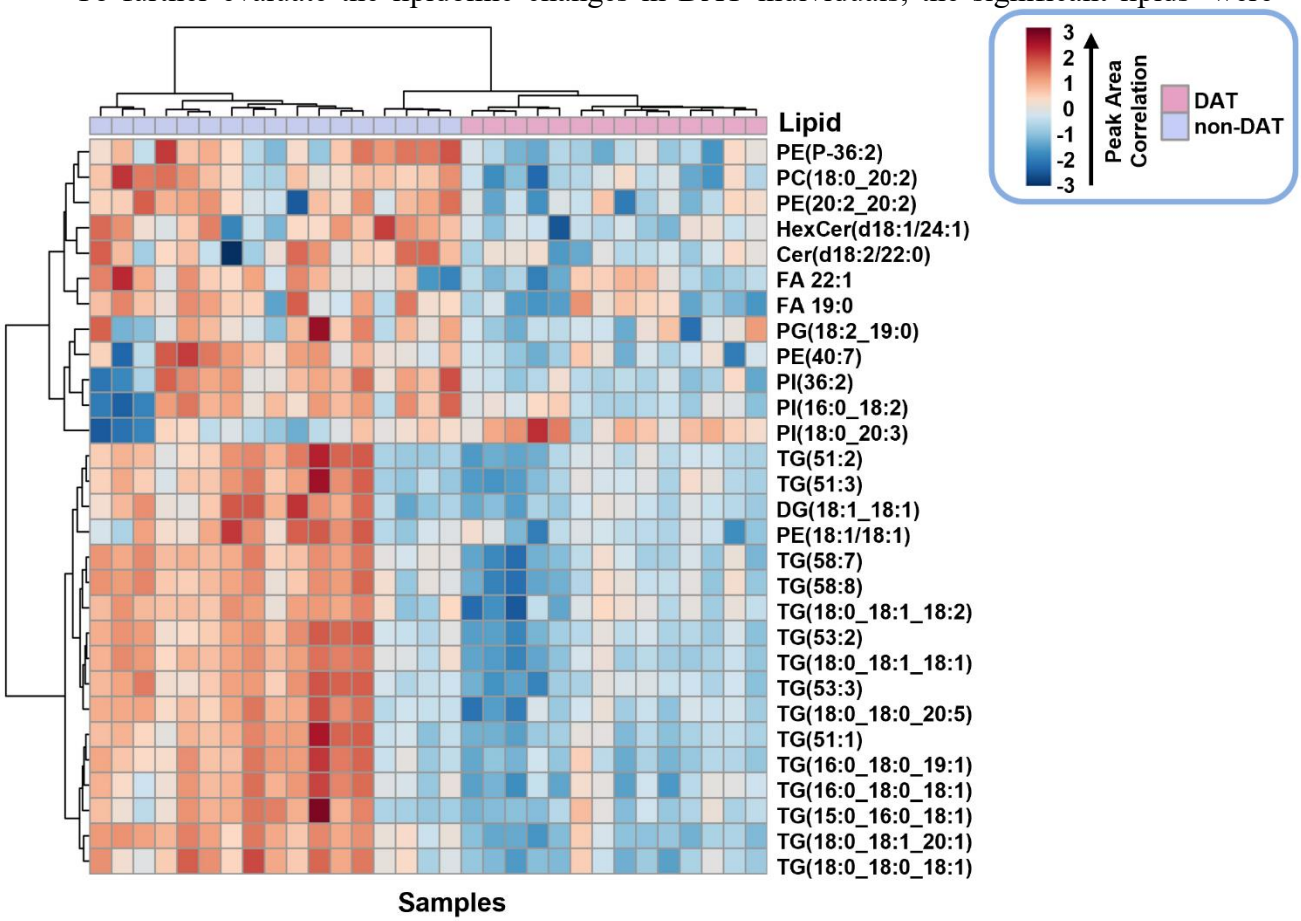

Figure 5. Hierarchical clustering of the California sea lion plasma samples for significant lipids detected in both positive and negative mode. Only the significant lipids are shown in each mode. Lipids with higher abundances are shown in red and those with less abundant in blue. The Euclidean distances were calculated and clustered using the Ward method.

359 assessed hierarchical clustering in Metaboanalyst 6.0[27](**Figure 5**). Here, hierarchical clustering
360 illustrated that the DAT and non-DAT individuals clustered, and similar trends were observed in

361 all glycerolipids, including the 15 TGs and 1 DG, plus 1 glycerophospholipid, PE(18:1/18:1).
362 Specifically, these lipids exhibit downregulation in the DAT samples, suggesting a link between
363 DAT and decreased TGs. Furthermore, many of the trending downregulated proteins are involved
364 with lipoprotein lipase, such as APOA1 and APOC2, which is responsible for the regulation of TG
365 degradation.[32] This further couples with the observed proteomic and lipidomic changes observed
366 in DAT. Interestingly, this was an unsupervised heatmap, thus the sample groups clustered
367 together without supervision. Consequentially, this clustering revealed another trend: four non-
368 DAT individuals had similar molecular compositions as those in the DAT group. Two of those
369 individuals were diagnosed with leptospirosis, another condition that is common among sea lions.[6]
370 One of those had trauma to the eye as well, which is worth noting because of the two that did not
371 have leptospirosis in that clustered group, one of them had flipper trauma. The last individual was
372 malnourished, which might explain why their abundance of TGs was lower than the rest of the
373 non-DAT individuals, since they may have had to rely on lipid energy stores to survive. The
374 malnourished individual is the left most sample in the heatmap, indicating that it clustered more
375 with the non-DAT samples. This illustrates a potential continuum between TG abundance and
376 DAT but requires further research to state conclusively.

377 To further probe lipid structure, trends in the degrees of unsaturation and fatty acyl chain
378 lengths were investigated to find patterns in the types of lipids found to be potential biomarkers
379 (**Figure 6**). Specifically, 58 % of the statistically significant lipids were found to have at least one
380 degree of unsaturation and 48 % had at least one fatty acyl chain with 18 carbons (considered long
381 chain fatty acids (LCFA)). Furthermore, diunsaturated lipids represented 9 % of the total lipids
382 detected but increased in representation to almost 18 % of the lipids found to be statistically
383 significant in DAT individuals. This 18-carbon fatty acyl chain and diunsaturation trend is further

384 supported by the volcano plot in **Figure 4**. Specifically, TG(18:0_18:1_20:1) which has two 18
385 carbon chains (all three LCFAs) and 2 double bonds has the lowest *p*-value (of the lipids with fatty
386 acyl chain assignments) and highest magnitude $\log_2$ fold change. Other statistically significant TGs
387 were also observed with 18 carbon chains and unsaturation (**Figure 5**), illustrating how TGs could
388 be quite informative of DAT in sea lions. The 15 statistically significant TGs downregulated in the
389 DAT group also support the idea that a simple TG blood panel assay could be developed for a
390 more accessible DAT evaluation platform, such as ultraviolet-visible spectroscopy. This would
391 enable rapid and affordable diagnostic testing for DAT and be extremely beneficial for the
392 veterinarians and sea lions.

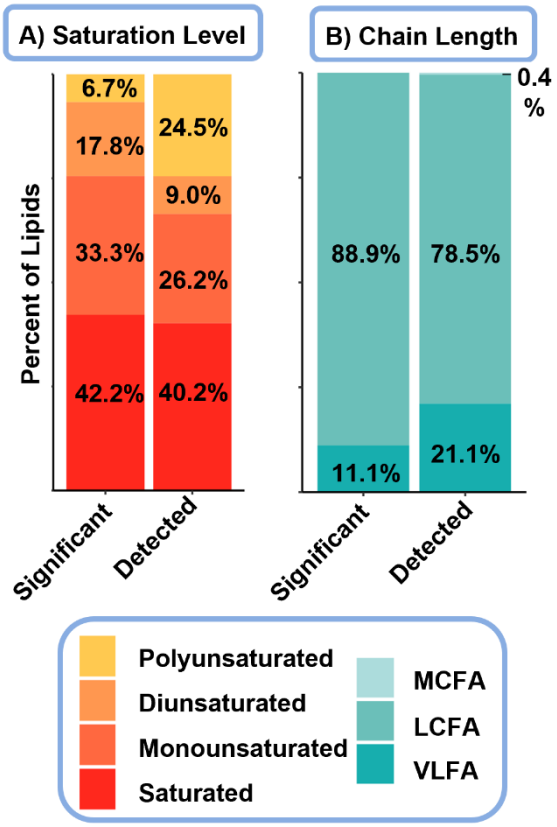

Figure 6. Saturation and chain length trends for detected and significant lipids in the DAT California sea lion plasma. **A)** The number of double bonds present in the fatty acyl chains of the significant and detected lipids, and **B)** variations in long chain fatty acids (13-20 carbons) or very long chain fatty acids (greater than 20 carbons). MCFA = medium chain fatty acids (6-12 carbons), LCFA = long chain fatty acids, and VLFA = very long chain fatty acids.

Although apolipoprotein and TG candidate biomarkers were determined in this work, this study does not go without limitations. First, the sample size of the study was only n = 31. This is a small group compared to the population of sea lions, especially considering the DAT group consisted of less than half of the total, n = 14. In addition to the study size, no healthy control group was present, as the non-DAT group had other ailments such as leptospirosis and starvation.[12]

399 However, healthy controls would be less useful for this study, as molecular markers for DAT are
400 specifically needed for diagnosis and the treatment of sick animals presenting with a specific set
401 of symptoms. Thus, future work using a larger sample size with more illnesses represented in the
402 non-DAT group as well as true healthy controls would be important for confirming the results
403 found in this study.
404

405 **CONCLUSIONS**

406 In this study, multi-omic analyses were conducted on California sea lion plasma to identify
407 potential biomarkers as diagnostic tools for DAT. The proteomic analyses confirmed APOE as a
408 DAT plasma biomarker from a previous study[12] and showcased 2 other apolipoproteins as
409 statistically significant and downregulated in the DAT sea lion plasma. In addition, 8 other
410 apolipoproteins were noted as having specific trends in the analyses but were not noted as
411 statistically significant, potentially because of the small sample size.[12] Lipidomic analyses of the
412 plasma further illustrated the effects of apolipoprotein dysregulation in 15 TGs, which are
413 associated with these proteins in the literature and were found to be less abundant in the sea lions
414 with DAT as well as four non-DAT with similar symptoms. Since the TGs made up over 50 % of
415 the significant lipids, they also provide a molecular class of interest that could be assayed (either
416 with LC-MS or a less complex, but robust instrument such as UV-Vis) by veterinarians in
417 conjunction with clinical signs such as seizures to provide a rapid diagnostic assessment. Although
418 a larger study would help validate our findings, the proteins and lipids noted to differentiate DAT
419 from non-DAT animals are extremely important for both understanding DAT molecular
420 perturbations and creating potential diagnostic and treatment strategies.

421

ACKNOWLEDGEMENTS

This work was funded by grants from the National Institute of Environmental Health Sciences (P42 ES027704), the National Institute of General Medical Sciences (R01 GM141277 and RM1 GM145416), and a cooperative agreement with the Environmental Protection Agency (STAR RD 84003201). This research was supported in part by the Intramural Research Program of the NIH (ZIC ES103363). The views expressed in this manuscript do not reflect those of the funding agencies. Identification of certain commercial equipment, instruments, software, or materials does not imply recommendation or endorsement by the National Institute of Standards and Technology, nor does it imply that the products identified are necessarily the best available for the purpose. We wish to thank Jackson Eberwein for his technical assistance related to sample preparation for proteomic analysis.

REFERENCES

(1) Ferrante, M. I.; Broccoli, A.; Montresor, M. The pennate diatom *Pseudo-nitzschia multistriata* as a model for diatom life cycles, from the laboratory to the sea. *Journal of Phycology* **2023**, *59* (4), 637-643. DOI: 10.1111/jpy.13342.

(2) Brunson, J. K.; Mckinnie, S. M. K.; Chekan, J. R.; Mccrow, J. P.; Miles, Z. D.; Bertrand, E. M.; Bielinski, V. A.; Luhavaya, H.; Oborník, M.; Smith, G. J.; et al. Biosynthesis of the neurotoxin domoic acid in a bloom-forming diatom. *Science* **2018**, *361* (6409), 1356-1358. DOI: 10.1126/science.aau0382.

(3) Pulido, O. M. Domoic Acid Toxicologic Pathology: A Review. *Marine Drugs* **2008**, *6* (2), 180-219. DOI: 10.3390/md20080010.

(4) Lefebvre, K. A.; Robertson, A. Domoic acid and human exposure risks: A review. *Toxicon* **2010**, *56* (2), 218-230. DOI: 10.1016/j.toxicon.2009.05.034.

(5) Gulland, E. M. D.; Haulena, M.; Fauquier, D.; Lander, M. E.; Zabka, T.; Duerr, R.; Langlois, G. Domoic acid toxicity in Californian sea lions (*Zalophus californianus*): clinical signs, treatment and survival. *Veterinary Record* **2002**, *150* (15), 475-480. DOI: 10.1136/vr.150.15.475.

(6) McClain, A. M.; Field, C. L.; Norris, T. A.; Borremans, B.; Duignan, P. J.; Johnson, S. P.; Whoriskey, S. T.; Thompson-Barbosa, L.; Gulland, F. M. D. The symptomatology and diagnosis of domoic acid toxicosis in stranded California sea lions (*Zalophus californianus*): a review and

evaluation of 20 years of cases to guide prognosis. *Frontiers in Veterinary Science* **2023**, *10:1245864*, . DOI: 10.3389/fvets.2023.1245864.
(7) Goldstein, T.; Mazet, J. A. K.; Zabka, T. S.; Langlois, G.; Colegrove, K. M.; Silver, M.; Bargu, S.; Van Dolah, F.; Leighfield, T.; Conrad, P. A.; et al. Novel symptomatology and changing epidemiology of domoic acid toxicosis in California sea lions (*Zalophus californianus*): an increasing risk to marine mammal health. *Proceedings of the Royal Society B: Biological Sciences* **2008**, *275* (1632), 267-276. DOI: 10.1098/rspb.2007.1221.

(8) Teitelbaum, J. S.; Zatorre, R. J.; Carpenter, S.; Gendron, D.; Evans, A. C.; Gjedde, A.; Cashman, N. R. Neurologic Sequelae of Domoic Acid Intoxication Due to the Ingestion of Contaminated Mussels. *New England Journal of Medicine* **1990**, *322* (25), 1781-1787. DOI: 10.1056/nejm199006213222505.
(9) Yang, K.; Han, X. Lipidomics: Techniques, Applications, and Outcomes Related to Biomedical Sciences. *Trends in Biochemical Sciences* **2016**, *41* (11), 954-969. DOI: 10.1016/j.tibs.2016.08.010.
(10) Aslam, B.; Basit, M.; Nisar, M. A.; Khurshid, M.; Rasool, M. H. Proteomics: Technologies and Their Applications. *Journal of Chromatographic Science* **2017**, *55* (2), 182-196. DOI: 10.1093/chromsci/bmw167.
(11) Neely, B. A.; Soper, J. L.; Gulland, F. M. D.; Bell, P. D.; Kindy, M.; Arthur, J. M.; Janech, M. G. Proteomic analysis of cerebrospinal fluid in California sea lions (*Zalophus californianus*) with domoic acid toxicosis identifies proteins associated with neurodegeneration. *PROTEOMICS* **2015**, *15* (23-24), 4051-4063. DOI: 10.1002/pmic.201500167.
(12) Neely, B. A.; Ferrante, J. A.; Chaves, J. M.; Soper, J. L.; Almeida, J. S.; Arthur, J. M.; Gulland, F. M. D.; Janech, M. G. Proteomic Analysis of Plasma from California Sea Lions (Zalophus californianus) Reveals Apolipoprotein E as a Candidate Biomarker of Chronic Domoic Acid Toxicosis. *PLOS ONE* **2015**, *10* (4), e0123295. DOI: 10.1371/journal.pone.0123295.
(13) Deutsch, E. W.; Bandeira, N.; Perez-Riverol, Y.; Sharma, V.; Carver, J., Jeremy; Mendoza, L.; Kundu, D. J.; Wang, S.; Bandla, C.; Kamatchinathan, S.; et al. The ProteomeXchange consortium at 10 years: 2023 update. *Nucleic Acids Research* **2023**, *51* (D1), D1539-D1548. DOI: 10.1093/nar/gkac1040.
(14) Perez-Riverol, Y.; Bai, J.; Bandla, C.; García-Seisdedos, D.; Hewapathirana, S.; Kamatchinathan, S.; Kundu, J., Deepti; Prakash, A.; Frericks-Zipper, A.; Eisenacher, M.; et al. The PRIDE database resources in 2022: a hub for mass spectrometry-based proteomics evidences. *Nucleic Acids Research* **2022**, *50* (D1), D543-D552. DOI: 10.1093/nar/gkab1038.
(15) Kong, A. T.; Leprevost, F. V.; Avtonomov, D. M.; Mellacheruvu, D.; Nesvizhskii, A. I. MSFragger: ultrafast and comprehensive peptide identification in mass spectrometry–based proteomics. *Nature Methods* **2017**, *14* (5), 513-520. DOI: 10.1038/nmeth.4256. Teo, G. C.; Polasky, D. A.; Yu, F.; Nesvizhskii, A. I. Fast Deisotoping Algorithm and Its Implementation in the MSFragger Search Engine. *Journal of Proteome Research* **2021**, *20* (1), 498-505. DOI: 10.1021/acs.jproteome.0c00544.
(16) Nesvizhskii, A. I.; Keller, A.; Kolker, E.; Aebersold, R. A Statistical Model for Identifying Proteins by Tandem Mass Spectrometry. *Analytical Chemistry* **2003**, *75* (17), 4646-4658. DOI: 10.1021/ac0341261.
(17) Yu, F.; Haynes, S. E.; Nesvizhskii, A. I. IonQuant Enables Accurate and Sensitive Label-Free Quantification With FDR-Controlled Match-Between-Runs. *Molecular & Cellular Proteomics* **2021**, *20*, 100077. DOI: 10.1016/j.mcpro.2021.100077.

(18) Peart, C. R.; Williams, C.; Pophaly, S. D.; Neely, B. A.; Gulland, F. M. D.; Adams, D. J.; Ng, B. L.; Cheng, W.; Goebel, M. E.; Fedrigo, O.; Haase, B.; Mountcastle, J.; Fungtammasan, A.; Formenti, G.; Collins, J.; Wood, J.; Sims, Y.; Torrance, J.; Tracey, A.; Howe, K.; Rhie, A.; Hoffman, J. I.; Johnson, J.; Jarvis, E. D.; Breen, M.; Wolf, J. B. W. Hi-C scaffolded short- and long-read genome assemblies of the California sea lion are broadly consistent for syntenic inference across 45 million years of evolution. *Mol. Ecol. Resour.* **2021**, 21 (7), 2455–2470. DOI: 10.1111/1755-0998.13443.

(19)Wickham, H.; Averick, M.; Bryan, J.; Chang, W.; McGowan, L.; François, R.; Grolemund, G.; Hayes, A.; Henry, L.; Hester, J.; et al. Welcome to the Tidyverse. *Journal of Open Source Software* **2019**, *4* (43), 1686. DOI: 10.21105/joss.01686. Kassambara, A. *rstatix: Pipe-Friendly Framework for Basic Statistical Tests* . . 2023. https://rpkgs.datanovia.com/rstatix/

(20) Folch, J.; Lees, M.; Stanley, G. H. S. A Simple Method for the Isolation and Purification of Total Lipides from Animal Tissues. *Journal of Biological Chemistry* **1957**, *226* (1), 497-509. DOI: 10.1016/S0021-9258(18)64849-5.

(21)Shang, X.; Du, J.; Zhao, Y.; Tian, J.; Jiang, S. Effect of Multiple Freeze-Thaw Cycles on Lipid Degradation and Lipid Oxidation of Grass Carp Surimi Containing Different Amounts of Pork Back Fat. *Food Science of Animal Resources* **2021**, *41* (6), 923-935. DOI: 10.5851/kosfa.2021.e46.

(22) Kirkwood, K. I.; Christopher, M. W.; Burgess, J. L.; Littau, S. R.; Foster, K.; Richey, K.; Pratt, B. S.; Shulman, N.; Tamura, K.; Maccoss, M. J.; et al. Development and Application of Multidimensional Lipid Libraries to Investigate Lipidomic Dysregulation Related to Smoke Inhalation Injury Severity. *Journal of Proteome Research* **2022**, *21* (1), 232-242. DOI: 10.1021/acs.jproteome.1c00820.

(23) Stow, S. M.; Causon, T. J.; Zheng, X.; Kurulugama, R. T.; Mairinger, T.; May, J. C.; Rennie, E. E.; Baker, E. S.; Smith, R. D.; Mclean, J. A.; et al. An Interlaboratory Evaluation of Drift Tube Ion Mobility–Mass Spectrometry Collision Cross Section Measurements. *Analytical Chemistry* **2017**, *89* (17), 9048-9055. DOI: 10.1021/acs.analchem.7b01729.

(24) Adams, K. J.; Pratt, B.; Bose, N.; Dubois, L. G.; St. John-Williams, L.; Perrott, K. M.; Ky, K.; Kapahi, P.; Sharma, V.; Maccoss, M. J.; et al. Skyline for Small Molecules: A Unifying Software Package for Quantitative Metabolomics. *Journal of Proteome Research* **2020**, *19* (4), 1447-1458. DOI: 10.1021/acs.jproteome.9b00640.

(25) MacLean, B.; Tomazela, D. M.; Shulman, N.; Chambers, M.; Finney, G. L.; Frewen, B.; Kern, R.; Tabb, D. L.; Liebler, D. C.; MacCoss, M. J. Skyline: an open source document editor for creating and analyzing targeted proteomics experiments. *Bioinformatics* **2010**, *26* (7), 966-968. DOI: 10.1093/bioinformatics/btq054.

(26) Kirkwood, K. I.; Pratt, B. S.; Shulman, N.; Tamura, K.; Maccoss, M. J.; Maclean, B. X.; Baker, E. S. Utilizing Skyline to analyze lipidomics data containing liquid chromatography, ion mobility spectrometry and mass spectrometry dimensions. *Nature Protocols* **2022**, *17* (11), 2415-2430. DOI: 10.1038/s41596-022-00714-6.

(27) Xia, J.; Psychogios, N.; Young, N.; Wishart, D. S. MetaboAnalyst: a web server for metabolomic data analysis and interpretation. *Nucleic Acids Research* **2009**, *37* (suppl_2), W652-W660. DOI: 10.1093/nar/gkp356.

541 (28) Clair, G.; Reehl, S.; Stratton, K. G.; Monroe, M. E.; Tfaily, M. M.; Ansong, C.; Kyle, J. E.
542 Lipid Mini-On: mining and ontology tool for enrichment analysis of lipidomic data.
543 *Bioinformatics* **2019**, *35* (21), 4507-4508. DOI: 10.1093/bioinformatics/btz250.
544 (29) D'Erasmo, L.; Di Costanzo, A.; Gallo, A.; Bruckert, E.; Arca, M. ApoCIII: A multifaceted
545 protein in cardiometabolic disease. *Metabolism* **2020**, *113*, 154395. DOI:
546 10.1016/j.metabol.2020.154395.
547 (30) Behbodikhah, J.; Ahmed, S.; Elyasi, A.; Kasselman, L. J.; De Leon, J.; Glass, A. D.; Reiss,
548 A. B.. Apolipoprotein B and Cardiovascular Disease: Biomarker and Potential Therapeutic
549 Target. Metabolites **2021**, 11 (*10*), 690. https://doi.org/10.3390/metabo11100690.
550 (31) Rouland, A.; Masson, D.; Lagrost, L.; Vergès, B.; Gautier, T.; Bouillet, B. Role of
551 apolipoprotein C1 in lipoprotein metabolism, atherosclerosis and diabetes: a systematic review.
552 *Cardiovascular Diabetology* **2022**, *21* (1). DOI: 10.1186/s12933-022-01703-5.
553 (32) Hsu, C.-C.; Kanter, J. E.; Kothari, V.; Bornfeldt, K. E. Quartet of APOCs and the Different
554 Roles They Play in Diabetes. *Arteriosclerosis, Thrombosis, and Vascular Biology* **2023**, *43* (7),
555 1124-1133. DOI: 10.1161/atvbaha.122.318290.
556 (33) Wang, X.; Musunuru, K. Angiopoietin-Like 3: From Discovery to Therapeutic Gene
557 Editing. *JACC: Basic to Translational Science* **2019**, *4* (6), 755-762. DOI:
558 10.1016/j.jacbts.2019.05.008.
559 (34) Kataoka, H.; Kawaguchi, M. Hepatocyte growth factor activator (HGFA):
560 pathophysiological functions *in vivo*. *The FEBS Journal* **2010**, *277* (10), 2230-2237. DOI:
561 10.1111/j.1742-4658.2010.07640.x.
562 (35) Manthey, H. D.; Cochain, C.; Busch, M.; Chaudhari, S. M.; Stegner, D.; Yepes, M.; Lorenz,
563 K.; Nolte, M. W.; Nieswandt, B.; Vorlova, S.; et al. Coagulation factor XII induces pro-
564 inflammatory cytokine responses in macrophages and promotes atherosclerosis in mice.
565 *Thrombosis and Haemostasis* **2017**, *117* (01), 176-187. DOI: 10.1160/th16-06-0466.
566 (36) Wang, C.; Yosef, N.; Gaublomme, J.; Wu, C.; Lee, Y.; Clish, B., Clary; Kaminski, J.; Xiao,
567 S.; Horste, Z., Meyer, Gerd; Pawlak, M.; et al. CD5L/AIM Regulates Lipid Biosynthesis and
568 Restrains Th17 Cell Pathogenicity. *Cell* **2015**, *163* (6), 1413-1427. DOI:
569 10.1016/j.cell.2015.10.068.
570 (37) Bárcena, C.; Aran, G.; Perea, L.; Sanjurjo, L.; Téllez, É.; Oncins, A.; Masnou, H.; Serra, I.;
571 García-Gallo, M.; Kremer, L.; et al. CD5L is a pleiotropic player in liver fibrosis controlling
572 damage, fibrosis and immune cell content. *EBioMedicine* **2019**, *43*, 513-524. DOI:
573 10.1016/j.ebiom.2019.04.052.
574 (38) Schymanski, E. L.; Jeon, J.; Gulde, R.; Fenner, K.; Ruff, M.; Singer, H. P.; Hollender, J.
575 Identifying Small Molecules via High Resolution Mass Spectrometry: Communicating
576 Confidence. *Environmental Science & Technology* **2014**, *48* (4), 2097-2098. DOI:
577 10.1021/es5002105.
578 (39) Epand, R. M. Features of the Phosphatidylinositol Cycle and its Role in Signal
579 Transduction. *The Journal of Membrane Biology* **2017**, *250* (4), 353-366. DOI: 10.1007/s00232-
580 016-9909-y.
581 (41) Sylvers-Davie, K. L.; Davies, B. S. J. Enzymes | Lipoprotein Lipase. In *Encyclopedia of*
582 *Biological Chemistry III (Third Edition)*, Jez, J. Ed.; Elsevier, 2021; pp 307-320.